Treatment Approaches For Enhancing Drug Delivery Using Mongolian Natural Zeolites

Altantogos Myagmar[1,2], Kader Poturcu[3], Ata Akcil[4,5], Ochirkhuyag Bayanjargal[1], Sarangerel Davaasambuu[6*]

[1] Department of Chemistry and Biological Engineering, National University of Mongolia (NUM), Ulaanbaatar, Mongolia
[2] Department of Medical Chemistry, Mongolian National University of Medical Sciences (MNUMS), Ulaanbaatar, Mongolia
[3] Department of Chemistry, Suleyman Demirel University (SDU), Isparta, Turkey
[4] Mineral-Metal Recovery and Recycling Research Group, Suleyman Demirel University (SDU), Isparta, Turkey
[5] Department of Mining Engineering, Nazarbayev University (NU), Astana, Republic of Kazakhstan
[6] Department of Chemistry, National University of Mongolia (NUM), Ulaanbaatar, Mongolia
[*]Corresponding author; Sarangerel Davaasambuu, Email: sarangerel@num.edu.mn

Abstract

Mongolia has substantial amounts of natural zeolite minerals, which hold considerable promise for environmental and biological uses, particularly located in the southeastern region of the country. To utilize Mongolian natural zeolite (MNZ) resources, this study focused on pretreating natural zeolite through acid activation, calcination, sodium exchange, and cationic surfactant modification to enhance its suitability for drug delivery. Each treatment step was successfully carried out, resulting in notable improvements in the physicochemical properties of Mongolian natural zeolite. Acid activation increased the surface area and removed impurities, while also contributing to a 46% increase in the Si/Al ratio. Calcination enhanced the structural stability of the framework, and sodium exchange further improved the ion-exchange capacity and biocompatibility of the zeolite. Finally, modification with the cationic surfactant played a significant role in increasing hydrophobicity and drug loading efficiency, as confirmed by FT-IR, XRD, SEM, and thermal analyses. Based on this adsorbent, the ceftriaxone delivery system showed effective and steadily increasing antibiotic release over time. These findings highlight the potential of pretreated Mongolian natural zeolite as a safe, efficient, and biocompatible carrier, serving as an effective adsorbent for drug delivery.

Keywords: Sulfuric acid activation; thermal treatment; drug delivery; biocompatibility; Si/Al ratio.

Introduction

Natural zeolites are crystalline, hydrated aluminosilicates with a well-defined porous structure, where the framework's negative charge is balanced by metal cations (M), owing to the presence of 4-valent silicon and 3-valent aluminum ions [1]. The chemical formula of zeolites, represented as $M_{x/n}[AlO_2]_x[SiO_2]_y \cdot zH_2O$, denotes n is the charge of the cation M, x+y as the total number of tetrahedra per unit cell, y/x as the Si/Al ratio, and z as the number of moles of water per unit cell [2]. Zeolites possess diverse framework structures with unique tetrahedral arrangements forming rings of 3, 4, 5, 6, 8, 10, and 12 members, resulting in various channel and cavity sizes. Pore sizes are typically classified by the number of ring members they contain: 8-membered rings for small pores, 10-membered rings for medium pores, and 12-membered rings for large pores [3]. Due to their versatile structural features and unique framework architecture characterized by varied tetrahedral arrangements, zeolites find extensive utility across diverse fields including petrochemistry [4], environmental remediation [5], and

pharmaceuticals [6], [7], catalysis [8], adsorption technology [9], construction materials [10], biomedical applications [11], agriculture [12], energy technology [13], and cosmetics [14].

One intriguing field of study that has attracted researchers' attention is the pharmaceutical application of zeolites, particularly as crucial components in pharmaceuticals, excipients, or drug delivery systems, specifically as carriers [15]. In drug delivery systems based on zeolites, fundamental characteristics such as pore size, Si/Al ratio, and hydrophobicity significantly influence loading capacity and the drug release process, thereby improving biocompatibility and efficiency [15]. As an example, Krajišnik et al. employed natural zeolite for delivering ibuprofen without pretreatment, with the natural zeolite having a Si/Al ratio of 5.59 and consisting primarily of clinoptilolite, along with traces of feldspar, quartz, and pyrite, thereby extending ibuprofen release to over 8 hours and releasing approximately 40% of the drug [16]. The study revealed significant efficiency limitations when using natural zeolite without pretreatment for drug delivery and highlighting the scarcity of untreated zeolite usage for this purpose. Pretreatment methods are emphasized due to the fundamental characteristic requirements for an effective natural zeolite-based drug delivery system. Pretreated zeolites are utilized to achieve controlled particle size and uniformity for predictable drug loading, enhancing drug loading capacity while maintaining structural integrity [17], designing precise controlled release kinetics [18], executing complex surface modifications without compromising stability [15], and ensuring stability in biological environments [19].

There are several research works that have used natural zeolite and employed a variety of pretreatment methods to enhance the properties of natural zeolites. These methods typically include acid activation, ion exchange, and combined approaches such as acid activation-thermal treatment, thermal treatment-acid activation, and ion exchange-thermal treatment for anticancer drugs, nonsteroidal anti-inflammatory drugs, antineoplastic agent, and antidiabetic medications. Kukobat et al. enhanced the properties of natural clinoptilolite zeolite from Croatia, through hydrochloric acid activation, which increased the surface area and pore volume, thereby improving the efficiency of the natural zeolite-based system as evidenced by facilitating up to 95% dissolution of the anticancer drug letrozole within 23 hours [20]. Likewise, through ion exchange pretreatment, experiments were conducted using a clinoptilolite-rich rock from California, USA, comprising approximately high content of clinoptilolite along with cristobalite, K-feldspar, trace amounts of quartz, and a micaceous phase, for diclofenac sodium delivery. After the ion exchange process, the Na_2O content increased from 3.32 wt % in natural zeolite to 6.51 wt % in ion-exchanged zeolite, and the Si/Al ratio changed only slightly. The results show that natural zeolite sustained drug release over about 5 hours, releasing 40% in the first hour, followed by a slower phase and a final rapid release. Ion exchange influenced this slower release, indicating drug absorption inside natural zeolite after surface exchange. Primarily driven by ion exchange, the drug predominantly adheres to the particle surface, involving stoichiometric ion exchange and mass transfer steps [21].

Moreover, some researchers used combined pretreatment methods to improve the structural and compositional properties of natural zeolite. Naimah et al. investigated Indonesian natural zeolite, composed of mordenite and clinoptilolite with minor quartz content, using the same drug as De Gennaro et al., but they employed combined pretreatments such as acid-thermal treatment. As a result, the activated zeolite showed significant improvements over natural zeolite, with the pore volume increasing by approximately 47% and the surface area increasing by about 46%. They studied diclofenac sodium release with the activated zeolite, where approximately 74% was released within 8 hours, matching the typical therapeutic dose duration [22]. In a one-hour interval, acid and thermal-treated zeolite improved efficiency by up to 52%, which was comparable to that of ion-exchanged zeolite for the same drug. Therefore, clinoptilolite obtained from the Mirsid quarry in Romania underwent mechanical, thermal, and chemical treatments to remove crystalline impurities while preserving its structure, followed by a two-step ion exchange process to obtain the monocationic forms Na^+ and H^+ [23]. Variations in compensatory cations, differing in size and hydration sphere, affected their occupancy within the pore system. The H^+ form exhibits a 50% larger surface area compared to the Na^+ form (33 $m^2 \cdot g^{-1}$ vs. 22 $m^2 \cdot g^{-1}$), highlighting their significant influence on NZ-based release systems. Bexarotene adsorbed on the monocationic H^+ system released 62% of the loaded drug in 18 hours, while the Na^+ system released only 26%, underscoring the significant impact of compensatory cations. The larger surface area of the H^+ form contributes to prolonged and controlled drug release [22]. Additionally, clinoptilolite-rich zeolites sourced from West Java, Indonesia, which were ion-exchanged and thermally treated, were used for delivering the antidiabetic medication metformin HCl. In the activated sample, there are no changes

observed in the diffraction patterns, indicating that the crystallinity of clinoptilolites remains unimpaired by NH_4Cl activation. However, activation with this combined treatment resulted in a significant increase in the BET surface area of clinoptilolite, rising from 48 $m^2 \cdot g^{-1}$ to 110 $m^2 \cdot g^{-1}$, attributed to the pretreatment process enhancing the surface area, total pore volume, and micropore volume of natural zeolite. The activation process effectively enriched the surface area of the clinoptilolite, crucial for improving its capacity to encapsulate drugs. The release of metformin HCl using this system achieved 83% within 7 hours and reached 85% by 12 hours, demonstrating sustained release characteristics [24]. The above-mentioned natural zeolites demonstrate their potential for drug delivery through various pretreatment methods, as shown by previous research, which significantly enhances their efficacy. The application of combined pretreatment methods, as evidenced by these results, underscores its versatility in enhancing drug delivery capabilities across a range of pharmaceuticals. In Mongolia, widespread antibiotic use poses significant challenges including antibiotic resistance and environmental pollution. To tackle these issues, we are exploring one of Mongolia's plentiful natural mineral resources for biomedical applications, specifically for drug delivery purposes involving subsequent treatments. Our goal is to improve the delivery efficiency of third-generation cephalosporins such as ceftriaxone (CFT) using pretreated natural zeolites, aiming to effectively address and contribute to challenges related to antibiotics.

Experiment

Materials

The natural clinoptilolite zeolite sample was collected from the Tushleg deposit in Mongolia, located at 44.5483° N, 109.9744° E. MNZ sample was first ground using a planetary ball mill (Retsch PM 400, Germany) and then sieved to obtain particles of 74 μm. The chemicals used in the study included sulfuric acid (H_2SO_4, ≥98.0 % purity), sodium chloride (NaCl, ≥99.5 % purity), and hexadecyltrimethylammonium bromide (HDTMA, ≥97.0 % purity), all of which were purchased from Merck KGaA, Germany. All chemicals were analytical grade and used as received. Ultrapure water produced by a Nuve ND 8 water distiller (Turkey) with a resistivity of at least 18 MΩ·cm at 25ºC was used to prepare all solutions, and the samples were subsequently stored at 4ºC.

Preparation and modification of natural zeolite for drug delivery

Several conventional methods were sequentially applied to modify MNZ zeolites, including sulfuric acid activation and calcination, ion exchange, and cationic surfactant modification. These modifications rendered the zeolites suitable for use in drug delivery.

Zeolite activation with sulfuric acid and calcination

Activation was carried out by refluxing the zeolite under varying sulfuric acid concentrations, followed by calcination. 40 g of MNZ powder were then combined with 800 mL of sulfuric acid solutions of varying concentrations (0.25 M, 0.5 M, and 1.0 M) that were stirred with a hot plate stirrer. The stirring was conducted on an MSH-200 digital hotplate stirrer (DAIHAN, Korea) at a speed of 1300 rpm for 30 minutes while maintaining a controlled temperature of 90ºC. The MNZ samples are collectively denoted as MNZ, with variants treated using sulfuric acid concentrations of 0.25 M, 0.5 M, and 1.0 M, referred to as MNZ-0.25, MNZ-0.50, and MNZ-1.0, respectively. After activation, the zeolite was washed with distilled water until the wash medium reached neutrality. The zeolite, air-dried for 24 hours, then underwent further treatment, including heating at 110ºC for 2 hours. Furthermore, following activation with sulfuric acid, the samples were subjected to calcination at 500ºC for 6 hours in a muffle furnace (M1811, Electromag, Turkey) [25]. This process ensured the effective preparation and treatment of the MNZ sample for the next step and facilitated the selection of the most effectively treated sample.

Sodium ion exchange

The experimental protocol was conducted following a previously reported paper with slight adjustments [26]. 10 g of natural zeolite were combined with a 0.5 M NaCl solution and stirred at 90ºC for 16 hours, and this procedure was repeated twice. The resulting mixture was subsequently washed with deionized water and left to dry for 24 hours at 25ºC. The zeolite samples were further placed in an oven at 110ºC to eliminate any hygroscopic moisture.

Cationic surfactant modification

10 g of sodium exchanged MNZ (MNZ-Na) were immersed in a 100 mL solution of 0.2 M HDTMA cationic surfactant, and the mixture was continuously stirred at 25ºC for 24 hours. The surfactant-exchanged sample was washed with deionized water until all free bromide ions were completely

removed, and no precipitate was observed upon the addition of an $AgNO_3$ solution. Lastly, the surfactant-modified zeolite was dried in an oven for 5 hours at 105ºC.

Characterization

The structural and compositional characteristics of the samples were evaluated through instrumental analyses, including X-ray fluorescence (XRF), X-ray diffraction (XRD), Fourier-transform infrared spectroscopy (FT-IR), and scanning electron microscopy (SEM), thermogravimetric/differential thermal analysis (TG/DTA).

Elemental analysis of the samples was performed using an Axios FAST simultaneous XRF spectrometer equipped with SuperQ software (PANalytical, UK). XRD analyses were conducted to determine the crystal structure, using a MAXima XRD-7000 instrument (Shimadzu, Japan) with Cu-Kα radiation. The diffraction patterns were analyzed using the Search/Match program with the JCPDS powder diffraction database for phase identification and sample characterization. FT-IR spectra were recorded on an IR Prestige-21 spectrophotometer over the range of 4000–400 cm^{-1} (Shimadzu, Japan).

The morphology and physical properties of the samples were characterized using a Field Emission Scanning Electron Microscope (QUANTA 400F, Thermo Fisher Scientific, USA) equipped with an energy dispersive X-ray (EDX) system, providing a high resolution of 1.2 nm and a magnification range from 40x to 300,000x. Additionally, the surface area and thermal properties were evaluated using a simultaneous TG/DTA analyzer (LABSYS evo, SDT650, Setaram Instruments, USA) under a controlled nitrogen atmosphere. The analysis spanned a temperature range of 25–1200ºC, with a heating rate of $10ºC \cdot min^{-1}$. These analyses were carried out to better understand the structure and composition of the zeolite samples, allowing for a thorough evaluation of their properties and potential applications.

Results

The MNZ sample, sourced from the Tushleg deposit in Mongolia, underwent activation and modification, and was then analyzed using instrumental techniques to determine its structural and compositional characteristics, yielding the following results. XRF spectroscopy determines the elemental composition of a sample, allowing for the identification of minerals and providing essential information about their mineralogical composition. The chemical composition of activated and sodium-exchanged MNZ samples was determined using XRF analysis, as presented in Table 1.

Table 1. XRF analysis of chemical constituents in treated samples

Chemical composition	Mass, %					
	MNZ	MNZ-1.0	MNZ-0.5	MNZ-0.25	MNZ-Ther	MNZ-Na
SiO_2	68.840	80.310	81.270	79.590	71.520	78.860
Al_2O_3	12.580	8.890	9.020	9.750	13.140	9.850
CaO	3.320	0.790	0.760	1.020	0.510	1.030
K_2O	2.170	1.630	1.440	1.660	2.900	1.130
Fe_2O_3	1.580	1.090	1.120	1.430	2.320	1.340
MgO	1.240	0.560	0.600	0.750	0.400	0.680
TiO_2	0.099	0.118	0.115	0.115	0.784	0.115
Na_2O	0.470	0.510	0.470	0.440	2.290	1.060
MnO	0.046	0.018	0.022	0.028	0.028	0.026
P_2O_5	0.027	0.004	0.002	0.004	0.022	0.006
Trace	<0.050	<0.050	<0.050	<0.050	<0.05	<0.05
LOI*	9.640	5.990	5.190	5.220	6.090	5.910
Si/Al**	*9.64*	15.92	*15.88*	14.39	9.50	14.11

*The loss on ignition; **The molar ratio of silicon to aluminum

The MNZ sample was strategically chosen based on previous studies conducted by the researchers on Mongolian zeolites, as it is a clinoptilolite-type zeolite with a high Si/Al ratio, making it suitable for a

variety of applications. The XRF characterization results show that the MNZ zeolite sample is primarily composed of SiO_2 (68.84 wt %) and Al_2O_3 (12.58 wt %), with a LOI of 9.64 wt %.

The MNZ sample has a Si/Al ratio of 9.64, and based on XRF results, it falls into the high-silica category, as zeolites are classified according to their Si/Al ratio [27]. The chemical composition of the zeolite framework, particularly the Si/Al ratio, plays a major role in determining its physicochemical characteristics. The performance of zeolites including their activity, selectivity, and stability is closely linked to both the Si/Al ratio and the distribution of aluminum within the framework. High-silica zeolites are employed in drug delivery systems due to their uniform pore structure, large surface area, and stability, which enable precise control over drug loading and release. The MNZ sample is suitable for our purpose, and after sulfuric acid activation, its Si/Al ratio is substantially increased. Acid activation of zeolite elevates the Si/Al ratio and unveils previously obstructed surfaces through effective dealumination. Deallumination in zeolites can vary depending on the specific framework T sites occupied by aluminum. The spatial arrangement and clustering of aluminum atoms influence their interatomic distances and the formation of cooperative active sites. Additionally, aluminum may be located on external surfaces, within internal channels, or at framework intersections, affecting the material's structural and catalytic properties. Acid treatment not only increases the Si/Al ratio, influencing acidity and pore size distribution, but also eliminates pore-blocking impurities, making it suitable for use in drug delivery systems [28].

The acid-activated zeolites are subjected to subsequent thermal treatment (calcination) at 500ºC. During calcination, structural and chemical transformations occur, including the removal of water molecules and volatile components, leading to increased stability and crystallinity. Thermal treatment of the MNZ-0.25 zeolite resulted in notable changes in its physicochemical properties. The Si/Al ratio decreased from 14.39 to 9.5, indicating partial dealumination and structural modifications within the zeolite framework. Based on previous studies, calcination at least 500ºC provides an optimal balance between surface area and structural stability, as the structural properties are preserved at this temperature. Calcination preserves the structural properties of the acid-activated zeolites and enhances cation mobility. However, high-temperature treatment at 500ºC transforms the cation-ordered phase into a cation-disordered phase. Additionally, variations in the content of other elements indicate cation redistribution and the possible removal of volatile components [29].

After calcination, sodium ion exchange was further applied in this study to improve the biocompatibility of MNZ-0.25. MNZ-Ther exhibited a Na_2O content of 2.29 wt %, whereas after MNZ-Na, the Na_2O content decreased to 1.060 wt %. During calcination, the zeolite framework and the positions of cations in the micro- and mesopores can change, which may lead to the loss of some Na^+ ions into the solution. This decrease is associated with the calcination-induced cation rearrangement and the replacement of Na^+ ions by other framework cations. Calcination also induces a phase transformation from a cation-ordered to a cation-disordered state, which further contributes to the reduction in overall Na_2O content [27]. This pretreatment provides an opportunity for improvement, especially when combined with cationic surfactants for the surface functionality, enabling the development of enhanced zeolite-based materials for targeted applications, such as drug delivery, with improved therapeutic efficacy and bioavailability [15].

XRD is a widely used technique in geology, materials science, and chemistry for identifying and analyzing the crystal structures of minerals. Fig. 1(a). presents the XRD patterns and FTIR spectra of MNZ and treated samples. The XRD and FT-IR spectra of MNZ-0.5 and MNZ-1.0 are presented in Fig. S1 and Fig. S2 XRD analysis of MNZ indicates that quartz (Q) is the predominant mineral, with minor amounts of muscovite (Mu), tridymite (T), albite (A), and microcline (Mi), and confirms that all the zeolites maintain a crystalline structure. Quartz exhibited peaks at 2θ angles of 20.84° and 26.63° (JCPDS card no. 46–1045), corresponding to the crystallographic planes (101) and (100), respectively. Muscovite exhibited peaks at 19.89°, 20.18°, 20.66°, 25.52°, 26.65°, 26.82°, 27.88°, 29.90°, 34.94°, 35.03°, 42.45°, and 55.86° (JCPDS card no. 07-0042), corresponding to the crystallographic planes (001), (001), (002), (200), (060), (020), (002), (201), (151), (061), (191), and (153), respectively. Tridymite peaks were observed at 20.47°, 20.54°, 23.18°, 23.23°, and 23.27° (JCPDS card no. 42-1401), corresponding to the crystallographic planes (101), (111), (211), (221), and (112), respectively. Albite showed peaks at 22.03°, 23.51°, 24.13°, 24.25°, 27.70°, 27.88°, 27.96°, 28.08°, 30.20°, and 35.00° (JCPDS card no. 9-0466), associated with the crystallographic planes (310), (211), (002), (310), (121), (122), (130), (221), (200), and (112), respectively. The similarity of the peak XRD patterns at the 2θ angle indicates that the materials share the same structure as described in D. Munkhbat et al [30]. After

acid activation, the intensity of quartz and other mineral peaks increased, indicating changes in the crystalline phases, as amorphous silicon became incorporated into the zeolite framework during the acid activation process, resulting in a more ordered and well-defined zeolite crystal structure. The degree of crystallinity of the zeolite also increased after acid activation. The H^+ ions preferentially attack the oxygen atoms bonded to aluminum rather than silicon, as the Al–O bond (116 kcal·mol^{-1}) has a much lower dissociation energy than the Si–O bond (190 kcal·mol^{-1}). It also helps eliminate surface and pore-blocking impurities while introducing hydrogen ions from acid to balance the charge deficiency within the zeolite framework. Al-O bonds are much easier to decompose than Si-O Since other acid-treated samples showed no significant differences, 0.25 M sulfuric acid concentration was chosen for further treatment to reduce reagent use and ensure environmental safety. The presence of acidic active sites gives zeolites strong hydrogenation and deoxygenation capabilities, while thermal treatment further enhances the stability and porosity of the acid-treated zeolite. Therefore, acid treatment is preferably conducted prior to calcination to optimize these properties. During calcination, water and organic molecules are removed without significant damage to the crystalline structure, resulting in increased porosity and surface area. For high Si/Al ratio zeolite, thermal treatment up to 500ºC does not cause significant structural changes detectable by XRD. Similar crystallinity losses upon thermal treatment have been reported for natural zeolites from Cuba, the Americas, and Romania [31]. No significant structural changes were observed during the sodium exchange process according to the XRD results. Overall, the zeolite framework remained intact throughout the treatments, indicating that the structure was neither altered nor destroyed.

Fig. 1. (a) XRD and (b) FT-IR analyses of MNZ and treated samples.

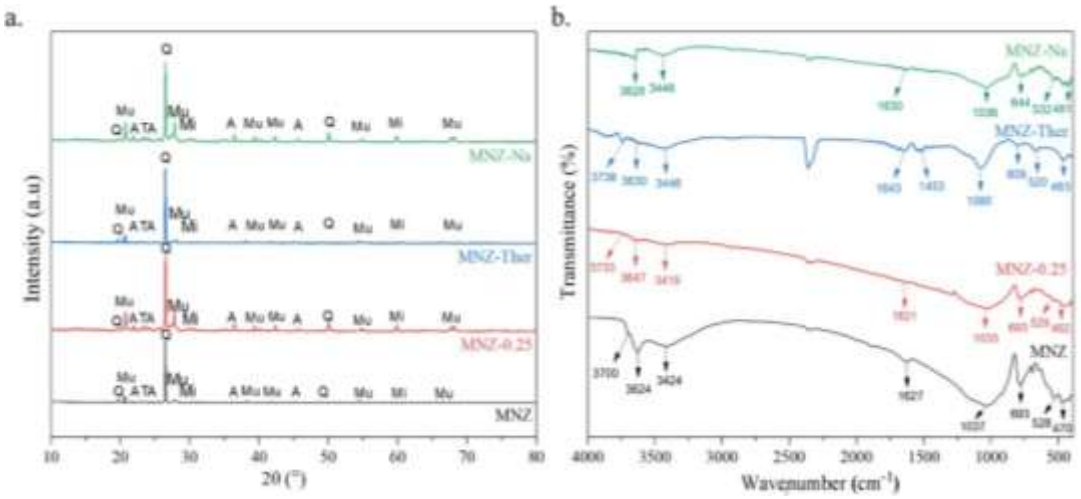

The infrared spectroscopic analysis of the samples reveals several distinct vibrational features, indicating the structural changes that occurred during the treatments (Fig. 1(b)). The spectral region between 400 and 800 cm^{-1} represents the Si–O bending vibrations of the zeolite framework and serves as a unique fingerprint, revealing the characteristic secondary building units that define its structure. The band observed at approximately 470 cm^{-1} corresponds to the internal rocking vibrations of T-O-T bridges, where T represents tetrahedral atoms, such as Si or Al. The bands at 528 cm^{-1} and 644 cm^{-1} are associated with bending deformations of Si-O bonds within the zeolite lattice and silicate structure, respectively. Furthermore, the strong peak observed at approximately 1037 cm^{-1} is also associated with Si-O stretching vibrations. However, this peak is more specifically attributed to the alterations in the positions of silicon and oxygen atoms within the zeolite's crystalline structure. Shifts or changes in the intensity of this peak can indicate significant structural rearrangements or modifications induced by the various treatments. High concentrations of H_2SO_4 used in the activation process can damage zeolite by causing decrystallization and increasing the amorphous phase due to the removal of aluminum from the zeolite framework.

When MNZ is treated with 0.25 M sulfuric acid, structural changes such as the removal of aluminum ions from the zeolite framework can be observed in the 1000–1100 cm^{-1} range, corresponding to the TO_4 [SiO_4] bond. This region is sensitive to Al–O or Si–O stretching vibrations. The characteristic broad

and intense peak at around 1037 cm^{-1} for MNZ decreases in intensity after acid activation, and a red shift is observed for MNZ-0.25 at 1035 cm^{-1}. This peak corresponds to asymmetric Si–O–Si stretching vibrations, which are also evident in this sample. The peak becomes broader and its intensity decreases relatively. This change is associated with the formation of more Si–O bonds and the occurrence of dealumination during acid activation. A similar trend is observed for the 0.5 M and 0.1 M acid-activated samples, as shown in the supplementary material [32].

For MNZ-Ther, the absorption peak at 1453 cm^{-1} in the infrared spectrum represents the Lewis acid sites of the zeolite. During calcination, the Lewis acidity of zeolites increases primarily due to surface dehydration or dehydroxylation and the formation of open metal sites. Calcination of zeolites at elevated temperatures can significantly modify their crystal framework and surface features. These thermal treatments may generate additional Lewis acid sites or strengthen existing ones by reorganizing the Si–O and Al–O bonds within the frameworo. As a result, zeolites treated at certain temperatures exhibit increased Lewis acidity due to the formation of more stable, highly reactive sites within the structure. In zeolites, thermal treatment serves to “activate” the material by generating framework defects and coordinatively unsaturated sites, which function as effective Lewis acid centers. By adjusting the calcination conditions, such as temperature and atmosphere, the number and strength of these acid sites can be carefully controlled [33].

The band at 3738 cm^{-1} corresponds to isolated silanol (Si–OH) groups located on the external surfaces of the particles. This characteristic peak is newly observed in the FTIR spectrum of MNZ-Ther and is typical of surface -OH groups. In the MNZ-Ther sample, the intensity of the 3738 cm^{-1} peak due to free silanols is notably reduced, whereas MNZ-0.25, which underwent desilication, exhibits a higher concentration of silanol groups. After calcination, this result is consistent with the XRF analysis, which revealed that the Si/Al ratio of MNZ-Ther decreased from 14.39 to 9.5, indicating structural changes within the zeolite framework. In all samples, the OH groups present in zeolites-which play a crucial role in their acidic properties-can be observed in the infrared spectra. The stretching vibrations of these –OH groups typically appear in the 3400–3600 cm^{-1} range, while their bending vibrations are detected in the 1600–1700 cm^{-1} region. The presence and intensity of these peaks serve as highly sensitive markers for tracking structural changes resulting from various treatments or activations. The peak at 1627 cm^{-1} and 3624 cm^{-1}, attributed to -OH groups, remain relatively stable during treatments, with the exception of thermal treatment, which may induce changes in the hydroxyl content or their local environment within the zeolite structure. By analyzing the changes in these vibrational features, researchers can gain insights into the structural transformations occurring in zeolitic materials upon acid activation and thermal treatment.

SEM data provide information on the surface morphology of natural and treated zeolites. The structural and morphological analysis of obtained zeolites was performed and the images are presented in Fig. 2. The zeolite samples MNZ, MNZ-Ther, and MNZ-Na exhibit shapeless and highly heterogeneous structures with rough surfaces, composed of irregular particles of various sizes and shapes characteristic for zeolites was observed. Notably, the MNZ-25 zeolite is denser compared to others.

Fig. 2. Surface morphology (a) MNZ, (b) MNZ-0.25, (c) MNZ-Ther, and (d) MNZ-Na.

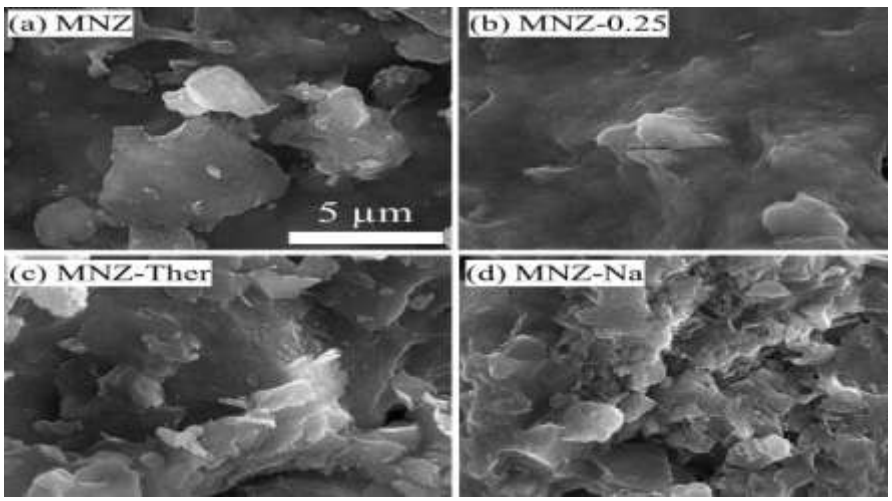

The structure of MNZ-Na was more irregular, and crystals were observed only locally, which is related to the sodium exchange process. Except for MNZ-Na, all samples exhibited a mesoporous structure with a possible presence of micropores. Additionally, the average particle size decreased progressively during both the calcination and sodium exchange treatments, suggesting that these processes contributed to structural refinement and particle size reduction.

Thermogravimetric analysis plays a crucial role in the comprehensive study of zeolites, enabling the precise evaluation of thermal stability, identification of loaded compounds, differentiation between dehydration and breakdown processes, and optimization for diverse applications. The thermal stability of natural and treated zeolites was examined using weight loss as a function of temperature, as shown in Fig. 3, highlighting the thermal responses of MNZ and its treated samples across the temperature range of 25–1200ºC (Fig. 3).

Fig. 3. TGA analysis of MNZ, MNZ-0.25, thermally treated, and sodium-exchanged samples.

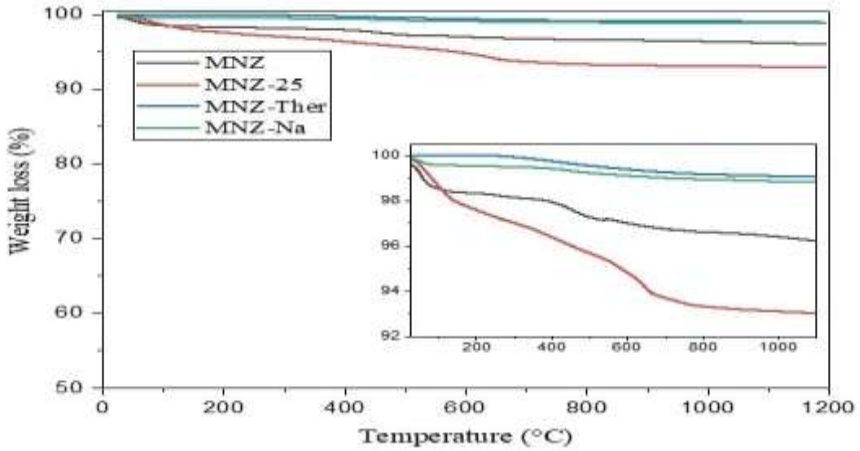

The weight loss of MNZ from 25 to 1200ºC was 3.92%, with distinct decreases: 1.5% (25-100ºC) due to hygroscopic water desorption, 1.65 % (100-200ºC) from removal of loosely bonded water, and 1.85% (200-300ºC) due to removal of loosely bound water. The weight loss decreases progressively at 300–400ºC (up to 2.05 %), 400–700ºC (up to 3.25%), and 700–1200ºC (up to 3.92%), which is attributed to zeolite framework dehydration, thermal instability of components, and desorption of adsorbed volatile compounds. The reduced mass loss in MNZ-Ther (0.92%) compared to MNZ (3.92%) is a result of the more extensive thermal treatment and removal of additional volatile compounds, indicating successful impurity and volatile substance removal [34]. For MNZ-Na weight loss is 1.2% and sodium ion exchange is a relatively cost-effective method for modifying zeolites, making it an attractive option for drug delivery systems where cost considerations are important.

Characterization of the MNZ-HDTMA

Cationic surfactants are widely used to enhance the adsorption capacity of zeolites for organic compounds [35], particularly drug adsorption [36], by modifying the surface properties. This surface modification reduces the negative charge and increases the hydrophobicity of the zeolite surface, thereby enhancing the adsorption of drug molecules [1]. MNZ-HDTMA, used as an adsorbent in the drug delivery system, was characterized using XRD, FTIR, TG/DTA, and SEM analyses as shown in Fig. 4. The MNZ-Na mineral structure is not changed during HDTMA modification, as observed in Fig. 4(a). The FTIR spectra after HDTMA modification are shown in Fig. 4(b). The FTIR peaks at approximately 2849 cm^{-1} and 2918 cm^{-1} in MNZ-HDTMA correspond to the symmetrical and asymmetrical C–H stretching vibrations of HDTMA's long alkyl chains, confirming the successful integration of HDTMA onto the natural zeolite [36], [37]. The peaks at 3420 cm^{-1} and 3042 cm^{-1} are due to the clinoptilolite lattice -OH stretching vibration, adsorbed H_2O deformation and H-OH bending vibration, respectively [38], [39].

Fig. 4. Characterization of MNZ–HDTMA using (a) XRD, (b) FT-IR, (c) TGA, and (d) SEM analyses.

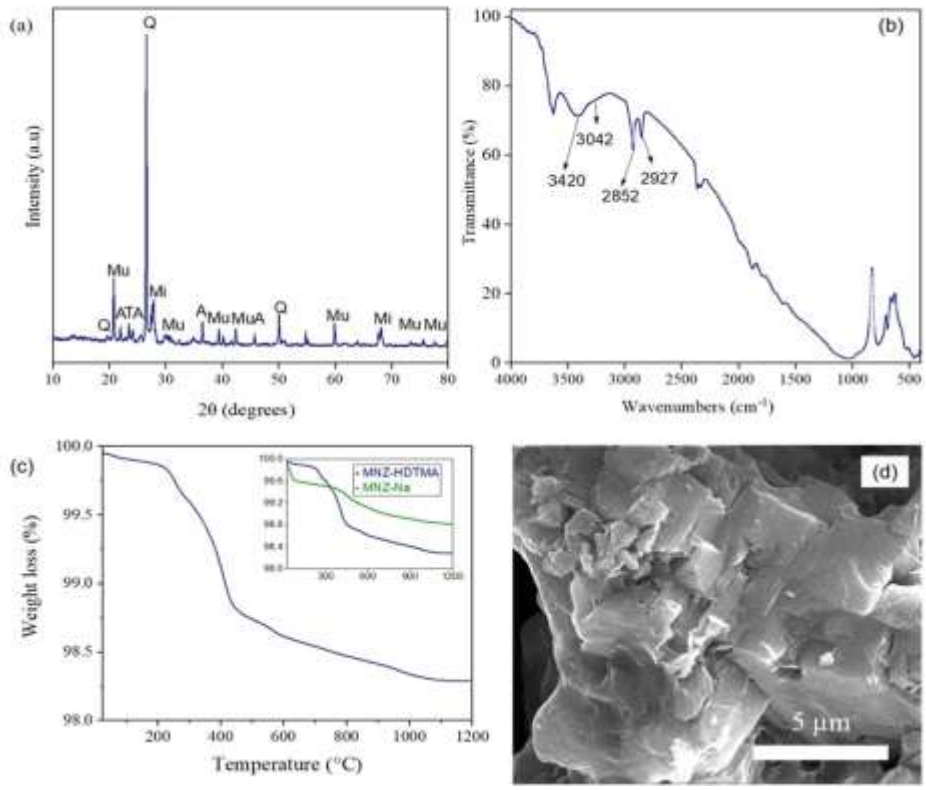

For MNZ-HDTMA in Fig. 4(c), there is an overall 1.7 % weight loss. A gradual 0.1% loss from 25 to 100°C due to the removal of externally bound water and a 0.15% change between 100ºC and 225ºC, which could be related to the gauche conformation of the surfactant's alkyl chain, as suggested by Sternik et al [40]. In the case of raw HDTMA, as reported by E.J. Sullivan et al., a substantial weight loss occurs, with nearly all HDTMA weight lost when heated to 232ºC [41]. At 235ºC, there's a significant 0.3% weight loss in HDTMA, attributed to the near melting point-related decomposition of HDTMA bromide and likely connected to the initiation of the defragmentation process of HDTMA molecules. For MNZ-HDTMA, there is a 1.2% weight loss recorded within the temperature bracket of 275 to 450ºC, and a subsequent 1.42% weight decrease in the 450 to 700ºC range, summing up to an overall 1.7% weight reduction spanning from 25 to 1200ºC. The 1.2% weight loss between 275 and 450°C is likely due to the desorption of HDTMA molecules or fragments, reflecting the reduced stability of HDTMA at higher temperatures. MNZ-Na has a 1.2% weight loss, while MNZ-HDTMA exhibits a more significant 1.7% weight loss, indicating effective HDTMA adsorption in MNZ-HDTMA, leading to increased weight loss in the latter case. In summary, the mass loss in MNZ-HDTMA observed at different temperature ranges can be attributed to the removal and desorption of HDTMA molecules and their degradation as the temperature increases. Overall, the characterization of the MNZ-HDTMA adsorbent confirms that the HDTMA modification was successful and suitable for use in a drug delivery system.

Using this adsorbent, the CFT delivery system was developed, and the cumulative release of the ceftriaxone antibiotic from the CFT@NZ-HDTMA system reached approximately 59%. The cumulative antibiotic release refers to the total amount of CFT that has been gradually released from the CFT@MNZ-HDTMA system over a specific period.

Fig. 5. Release pattern of ceftriaxone from the CFT@MNZ-HDTMA system.

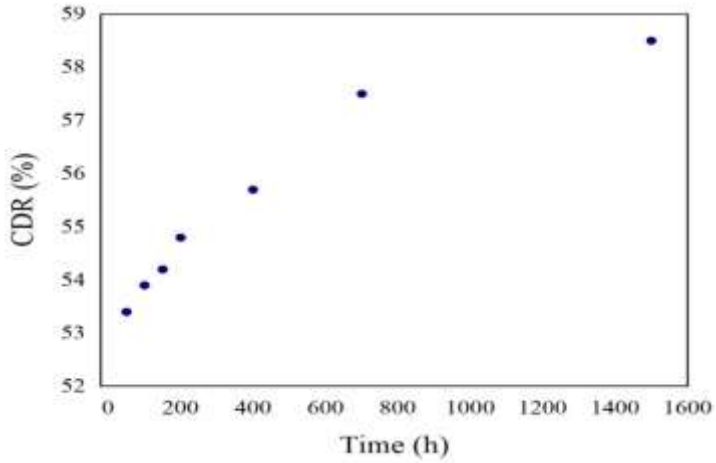

This release profile demonstrates a sustained and controlled release behavior, suggesting that the MNZ-HDTMA effectively regulates drug diffusion and can maintain therapeutic concentrations over an extended period. Thus, pretreated natural zeolites exhibit enhanced release performance, confirming their effectiveness as natural mineral-based carriers for drug delivery. Such modifications improve the structural and compositional properties of zeolites, thereby enhancing drug loading and release capacities and highlighting the great potential of natural zeolites as efficient and sustainable materials for advanced drug delivery systems.

Conclusion

As a result of the research, it can be concluded that MNZ from the Tushleg deposit in Mongolia is suitable as an abundant, high–Si/Al-ratio material for developing drug delivery systems, ensuring effective drug loading and release. Subsequent treatments, including acid activation, thermal treatment, sodium ion exchange, and cationic surfactant modification, significantly enhanced the physicochemical properties of MNZ, increasing the Si/Al ratio, structural stability, and biocompatibility. During the treatments, the Si/Al ratio of MNZ increased by approximately 46%, primarily due to sulfuric acid activation and sodium exchange, which improved the biocompatibility of the zeolite. Culminating in modification with the cationic surfactant HDTMA, the treatments were confirmed by FT-IR, XRD, SEM, and thermal analyses to be successful, also enhancing the hydrophobicity of the zeolite and improving drug loading efficiency without affecting its crystalline structure. These findings underscore the importance of using pretreatment methods to tailor zeolite properties effectively for pharmaceutical applications, while enhancing the MNZs' suitability by improving structural stability and moreover drug loading and release capabilities. These results demonstrate that pretreated natural zeolites, particularly when modified with cationic surfactants, are suitable for developing drug delivery systems.

References

[1] T. Derbe, S. Temesgen, M. Bitew: Advances in Materials Science and Engineering, 2021 (2021) 1–17.
[2] H. Ghobarkar, O. Schäf, U. Guth: Journal of Solid State Chemistry, 142 (1999) 451–454.
[3] E.M. Flanigen, H. Khatami, H.A. Szymanski: Infrared Structural Studies of Zeolite Frameworks, American Chemical Society (1974).
[4] I.C. Medeiros-Costa, E. Dib, N. Nesterenko, J.P. Dath, J.P. Gilson, S. Mintova: Chemical Society Reviews, 50 (2021) 11156–11179.
[5] I.E. Bojaddayni et al.: Minerals Engineering, 190 (2023) 1–20.
[6] E. Yee, S. Cheng, G. Knappe, C. Moomau: MIT Science Policy Review, 1 (2020) 10–17.
[7] I.M.S. Souza, C.I. Sainz-Díaz, C. Viseras, S.B.C. Pergher: Microporous and Mesoporous Materials, 292 (2020) 109733–109780.
[8] Y. Chai, W. Dai, G. Wu, N. Guan, L. Li: Accounts of Chemical Research, 54 (2021) 2894–2904.
[9] E. Pérez-Botella, S. Valencia, F. Rey: Chemical Reviews, 122 (2022) 17647–17695.
[10] J. Behin, E. Ghadamnan, H. Kazemian: Clay Minerals, 54 (2019) 131–144.
[11] C. Nomicisio et al.: Pharmaceutics, 15 (2023) 1–35.

[12] J. Szerement, A. Szatanik-Kloc, R. Jarosz, T. Bajda, M. Mierzwa-Hersztek: Journal of Cleaner Production, 311 (2021) 1–19.
[13] L. Kouchachvili, D.A. Bardy, R. Djebbar, L.V.E.W. Hogg: Journal of Porous Materials, 30 (2023) 163–173.
[14] A.P. Ferreira, C. Almeida-Aguiar, S.P.G. Costa, I.C. Neves: Molecules, 27 (2022) 8525–8525.
[15] G.T.M. Kadja, N.T.U. Culsum, R.M. Putri: Results in Chemistry, 5 (2023) 100910–100910.
[16] D. Krajišnik, A. Daković, A. Malenović, M. Kragović, J. Milić: Clay Minerals, 50 (2015) 11–22.
[17] I.M.S. Souza, F. García-Villén, C. Viseras, S.B.C. Perger: Pharmaceutics, 15 (2023) 1–33.
[18] G.T.M. Kadja, N.J. Azhari, S. Mardiana, N.T.U. Culsum, A. Maghfirah: Results in Engineering, 17 (2023) 100910–100910.
[19] N. Grifasi, B. Ziantoni, D. Fino, M. Piumetti: Environmental Science and Pollution Research, 31 (2024) 1–36.
[20] R. Kukobat et al.: Journal of Colloid and Interface Science, 653 (2024) 170–178.
[21] P. Cappelletti et al.: Microporous and Mesoporous Materials, 250 (2017) 232–244.
[22] K. Naimah: Kimia Sains dan Aplikasi, 24 (2021) 91–100.
[23] B. de Gennaro: Surface Modification of Zeolites for Environmental Applications, Elsevier (2018).
[24] W.A. Putra, I.G.A.W. Kusumawati: Asian Journal of Pharmaceutical and Clinical Research, 11 (2018) 285–289.
[25] J.L. Sihombing, S. Gea, A.N. Pulungan, H. Agusnar, B. Wirjosentono, Y.A. Hutapea: Journal of Physics: Conference Series, 2049 (2018) 1–8.
[26] S. Mishra, A. Akcil, S. Panda, I. Agcasulu: Energy and Fuels, 32 (2018) 2869–2877.
[27] N. Kordala, M. Wyszkowski: Molecules, 29 (2024) 1069–1075.
[28] J. Li, M. Gao, W. Yan, J. Yu: Chemical Science, 14 (2022) 1935–1959.
[29] Y. Goto et al.: Journal of Solid State Chemistry, 299 (2021) 122695–122698.
[30] D. Munkhbat, S. K, B. Ochirkhuyag: Mongolian Journal of Chemistry, 17 (2017) 50–54.
[31] S. Tanirbergenova et al.: Processes, 13 (2025) 1–19.
[32] D.Y. Lestari: Proceedings of the National Seminar on Chemistry and Chemistry Education, 32 (2010) 17–24.
[33] X. Wei et al.: Molecular Catalysis, 537 (2023) 112948–112952.
[34] N. Kamaly, B. Yameen, J. Wu, O.C. Farokhzad: Chemical Reviews, 116 (2016) 2602–2663.
[35] G.A. Gaynanova, L.A. Vasileva, E.A. Romanova, L.Y. Zakharova, O.G. Sinyashin: Journal of Molecular Liquids, 439 (2025) 128864–128868.
[36] D. Smiljanić et al.: Materials, 14 (2021) 1–18.
[37] M. Łach et al.: Materials, 15 (2022) 1–15.
[38] C. Wan, X. Cui, M. Liu, B. Xu, J. Sun, S. Bai: Molecules, 28 (2023) 1–21.
[39] A. Fajdek-Bieda, A. Wróblewska, P. Miądlicki, J. Tołpa, B. Michalkiewicz: Reaction Kinetics, Mechanisms and Catalysis, 133 (2021) 997–1011.
[40] D. Sternik, A. Gładysz-Płaska, E. Grabias, M. Majdan, W. Knauer: Journal of Thermal Analysis and Calorimetry, 129 (2017) 1277–1289.
[41] M.C. Díaz-Nava, M.T. Olguín, M. Solache-Ríos, M.T. Alarcón-Herrera, A. Aguilar-Elguezabal: Journal of Inclusion Phenomena and Macrocyclic Chemistry, 51 (2005) 231–240.